Hindawi
Advances in Condensed Matter Physics
Volume 2018, Article ID 4578148, 7 pages
https://doi.org/10.1155/2018/4578148

Research Article

Highly Efficient Broadband Light Absorber Based on Nonuniform Hyperbolic Metamaterial Film

Nina A. Zharova,[1] Alexander A. Zharov ,[2] and Alexander A. Zharov Jr.[2]

[1] *Institute of Applied Physics, Russian Academy of Sciences, Nizhny Novgorod 603950, Russia*
[2] *Institute for Physics of Microstructures, Russian Academy of Sciences, Nizhny Novgorod 603950, Russia*

Correspondence should be addressed to Alexander A. Zharov; zharov@ipmras.ru

Received 9 January 2018; Accepted 3 May 2018; Published 3 June 2018

Academic Editor: Charles Rosenblatt

We develop a concept of highly efficient broadband light absorber based on nonuniform hyperbolic metamaterial. We suggest a gradual bending of the anisotropy axis inside the metamaterial that results in spatial shift of the area of resonant absorption depending on the incidence angle. In this resonant region the wavevector of light is parallel to the generatrix of resonant cone and the radiation losses are maximal because of extremely high value of refraction index. Changing the radiation frequency also shifts the spatial position of the resonant region so that high level of absorption may be achieved in wide frequency range. Using the model of nanowire medium (silver wires in silica host) we predict that 200 nm film of this hyperbolic metamaterial allows reaching almost total absorption of radiation throughout the visible band.

1. Introduction

Exotic and interesting electromagnetic properties of the so-called hyperbolic metamaterials (HMs) cause their extensive study [1–7]. HM is an anisotropic resonance medium with hyperboloid-shaped isofrequency surface. In optics HM can be realized, for example, as a metal-dielectric planar nanostructure or a lattice of metallic nanowires embedded in a dielectric matrix.

The ability to support high-index volume electromagnetic modes is one of the main advantages of HM, and it results from the subwavelength light localization, which is also a characteristic feature of surface plasmon polaritons. The similarity comes from the fact that the volume electromagnetic mode in HM is actually the superposition of interacting plasmon modes localized at the nearby metal-dielectric interfaces. The collective character of the modes results in a hybridized broadband response [8, 9].

Unique properties of HM can lead to a wide variety of applications; among these are negative refraction [10, 11], subwavelength imaging [12–17], spontaneous and thermal emission engineering [18–21], and broadband light trapping [22, 23]. Very high density of photonic states in HM [24–26] ensures effective radiative heat transfer [4–6] and allows for a *nanosized* heating/cooling devices.

Hyperbolic character of the metamaterial (MM) can be achieved only for rather high volume fraction of metal that causes high losses. The radiation absorption is especially strong in the case of high refractive index, when a wave beam propagates with its phase velocity directed along the resonance cone generatrix. Unavoidable ohmic loss is a great drawback for applications in high-resolution imaging and lithography; however this effect can be used to engineer absorbing coatings.

The functionality of the absorber (let it be an absorbing film) is defined by its absorptivity, its spatial extent (preferably, smallest), and its broadband and omnidirectional operation. The absorptivity, in turn, depends on the thickness of the film, on the radiation wavelength, and on the incidence angle. In the case of anisotropic material of the film one can also consider the orientation of the anisotropy axis. Some of the requirements are contradictory. Indeed, thin films often demonstrate resonant behaviour that leads to strong angular and wavelength dependence of the absorption coefficient; severely absorbing material with large imaginary part of the permittivity (able to absorb the radiation in small volume)

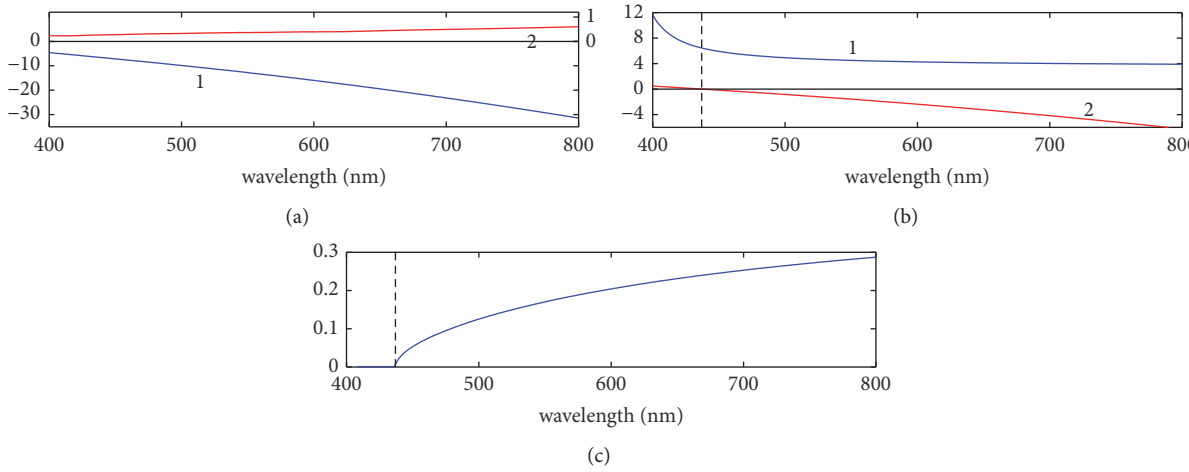

Figure 1: (Color online) (a) the wavelength dependence of real (curve 1) and imaginary (curve 2) parts of the permittivity of silver, ε_M (notice different scales for $\mathrm{Re}(\varepsilon_M)$ and $\mathrm{Im}(\varepsilon_M)$); (b) the dispersion of dielectric tensor components (real part) $\varepsilon_\parallel$ (curve 1) and $\varepsilon_\perp$ (curve 2) of effective wire medium (silver wires with volume fraction $\rho_M = 0.25$ in silica host); (c) the normalized critical angle, ϕ^*/π as a function of the wavelength. Dashed line marks the transition from common elliptical medium to the hyperbolic one with $\varepsilon_\parallel \varepsilon_\perp < 0$.

strongly reflects the incident wave. These contradictions make it difficult to design an absorber.

The engineering problem is twofold: first, it is necessary to avoid strong reflection when launching light from free space, and second, it is desirable to transform the incident light into small-scale radiation which is strongly damped and can be almost totally absorbed in a quite *thin* MM layer.

Usual way to improve the coupling between free space radiation and the medium is a modification of the air-medium interface, for example, using a diffraction grating. If the grating period is less than the wavelength in free space, then the scattered small-scale radiation can be effectively absorbed in the metamaterial. An interesting approach for increasing the absorption in hyperbolic media was proposed in [27] where the authors experimentally observed strongly reduced reflection from roughened metamaterial surface.

Another approach for increasing the absorption is to turn the optical axis of HM in such a way that the direction of the resonance cone generatrix would coincide with the normal to the HM interface [5–7]. In this case normally incident light directly transforms into small-scale radiation; however, rather high reflection takes place (see Figure 4) which has a detrimental effect on the absorptivity of the HM layer. In both cases, the spatial spectrum of radiation is changed mainly at the interfaces. On the other hand, the absorption can be increased due to the medium inhomogeneity.

2. Statement of the Problem

In this paper, we study the absorbing properties of the HM layer when the material structure changes inside the slab. We use the effective medium approximation and consider the propagation of the extraordinary wave in the wire medium: dielectric host with metal wires. In this case the components of effective permittivity tensor $\hat{\varepsilon}$ along the wires $\varepsilon_\parallel$ and perpendicular to them $\varepsilon_\perp$ can be defined as [28]

$$\begin{aligned} \varepsilon_\parallel &= \varepsilon_M \rho_M + \varepsilon_D (1 - \rho_M) \\ \varepsilon_\perp &= \varepsilon_D \frac{\varepsilon_M (1 + \rho_M) + \varepsilon_D (1 - \rho_M)}{\varepsilon_D (1 + \rho_M) + \varepsilon_M (1 - \rho_M)}, \end{aligned} \tag{1}$$

where ε_D is the permittivity of dielectric host, ε_M is the permittivity of metal, and ρ_M is the volume fraction of metal. Below we limit ourselves to the TM polarization of the light and use for computations the parameters of silica ($\varepsilon_D = 2.1590$) and silver with the volume fraction $\rho_M = 0.25$. The dispersion dependence of silver $\varepsilon_M(\lambda)$ is taken from [29] and depicted in Figure 1(a): notice different scales for real and imaginary parts of permittivity.

Figure 1 shows also the dependence of $\varepsilon_\parallel$, $\varepsilon_\perp$ (see Figure 1(b)), and the normalized critical angle, ϕ^*/π (see Figure 1(c)), on the radiation wavelength; the latter can be found from the condition $\tan(\phi^*) = \mathrm{Re}(\sqrt{-\varepsilon_\parallel/\varepsilon_\perp})$. ϕ^* is the angle of the resonance cone opening: the hyperbolic medium is transparent only for the waves with the wave vector $\mathbf{k}$ inside the resonance cone, i.e., when the angle between the optical axis $\mathbf{s}$ of the MM and $\mathbf{k}$ is less than ϕ^*, $\angle(\mathbf{k}, \mathbf{s}) \leq \phi^*$. The refraction index for normally incident light tends to infinity when the longitudinal (along the wires) optical axis of the metamaterial makes an angle ϕ^* with the normal to the interface (the resonance cone generatrix is along the normal). Dashed line marks the critical wavelength ($\lambda^* \approx 437$ nm) at which the topological transition takes place: the effective medium transforms from common elliptical to hyperbolic state.

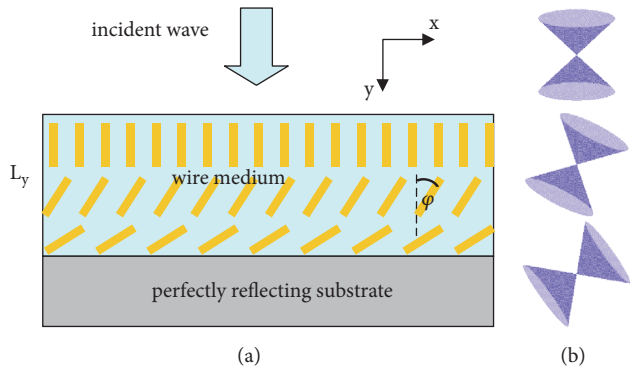

FIGURE 2: (Color online) (a) the geometry of the problem: the wire-medium slab with the thickness L_y is placed on the perfectly reflecting substrate. The components ε_{xx}, ε_{yy}, and ε_{xy} of the effective permittivity tensor depend on the orientation of the principal axes of the metamaterial, i.e., on the angle ϕ between the wires and the normal to the air-MM interface. In the slab of homogeneous metamaterial ϕ is fixed; however, we also consider the case of spatially changing orientation of the medium optical axis (see Figures 5–7). (b) Sketch of resonance cones orientation in inhomogeneous hyperbolic medium. The wave vector **k** of propagating radiation is located inside the resonance cone.

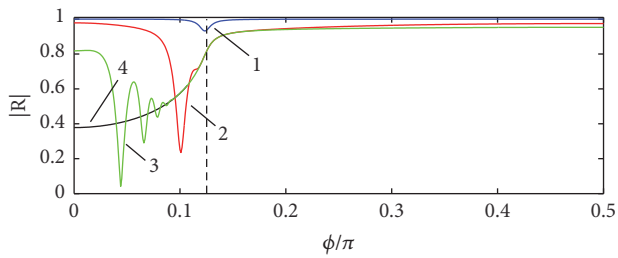

FIGURE 3: (Color online) the reflection coefficient at normal incidence as a function of the angle ϕ (see text). The dashed line indicates the specific angle $\phi = \phi^*$, at which the resonance cone generatrix is parallel to **n**. Lines 1, 2, and 3 correspond to the reflection from the uniform MM film (placed on the perfectly reflecting substrate) with the thickness $L_y^{(1)} = 10$ nm, $L_y^{(2)} = 100$ nm, and $L_y^{(3)} = 1000$ nm, and the line 4 corresponds to the reflection from the HM half-space. The wavelength of the radiation is 500 nm.

3. Reflection from Homogeneous HM Slab

In the following, we consider the reflection of incident radiation from the MM slab with the thickness L_y placed on the perfectly reflecting substrate. The geometry is shown in Figure 2.

Hyperbolic medium is highly anisotropic, and the wave propagation and, in particular, the reflection coefficient depend on the mutual arrangement of the incident light wave (vector **k**) and the metamaterial's normal **n** and symmetry axis **s**. In this paper, we consider reflection from a uniform slab with fixed orientation of the optical axis, $\angle(\mathbf{n}, \mathbf{s}) \equiv \phi = \text{const}$, and reflection from the MM slab in which ϕ varies linearly with the coordinate y.

Figure 3 shows the dependence of the reflection coefficient on the angle ϕ in the case of the uniform slab. The results are given for three values of the film thickness, $L_y^{(1,2,3)} = 10$, 100, and 1000 nm, and also for the reflection from the HM half-space, $L_y^{(4)} = \infty$. One can see that for the angles $\phi \approx \phi^*$ the curves 2, 3, and 4 nearly coincide. This means that rather thin MM films behave as (infinitely) thick ones when the relation $\phi = \phi^*$ is satisfied. This statement is verified for most of the visible domain, as one can see in Figures 4(a) and 4(b) (curves 3).

Figure 4 shows the spectral dependence of absorption of normally incident light. Solid lines in the panel (a) show the wavelength dependence of the absorption coefficient $D = 1 - |R|^2$ (R is the reflection coefficient, i.e., the ratio of the complex amplitudes of reflected and incident waves) in the case of metamaterial layer of finite thickness $L_y = 200$ nm, while the dotted lines correspond to the absorption coefficient $D_\infty = 1 - |R_\infty|^2$ of the MM half-space. The orientation angle is $\phi = 0$ (curve 1), $\phi = 0.1\pi$ (curve 2), and $\phi = \phi^*$ (curve 3; note that ϕ^* also depends on λ, see Figure 1(c)). Panel (b) demonstrates the wavelength dependence of the ratio D/D_∞ for these three cases. One can see that a thin layer with $\phi = \phi^*$ absorbs as an infinite one (the curve 3 actually coincides with the corresponding dotted line in panel (a) and the ratio $D/D_\infty = 1$ in the whole visible band), but considerable part of radiation is reflected. The absorption of the finite layer with fixed orientation angle (curves 1, 2) strongly depends on the wavelength and degrades for longer waves.

4. Nonuniform Absorber

Weak wavelength dependence of absorption is attractive for broadband operation, but it is achieved only for specific choice of the angle $\phi = \phi^*(\lambda)$ (curve 3 in Figures 4(a) and 4(b)). Certainly, such an absorber with the optical axis turning in accordance with the wavelength is unrealistic. However, the absorbing properties can be improved for the case of *nonuniform* film. For simplicity we consider the metamaterial with constant ρ_M and suppose that the orientation angle ϕ increases linearly (from 0 to $\pi/2$) with the propagation length. These situation cannot be achieved in common wire medium since changing the orientation of the wires changes also the density of wires and thus the value of ρ_M. On the other hand, within the effective medium

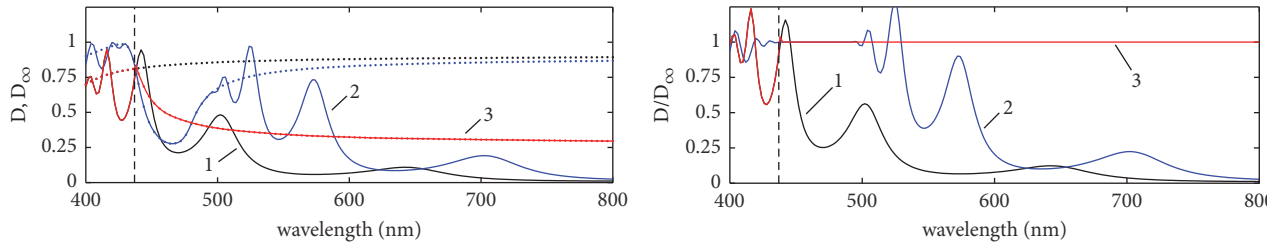

(a) (b)

FIGURE 4: (Color online) (a) the absorption coefficient $D = 1 - |R|^2$ (solid lines) of the uniform MM layer of finite thickness $L_y = 200$ nm at normal incidence as a function of the wavelength. Dotted lines show the absorption coefficient $D_\infty = 1 - |R_\infty|^2$ for the wave incident onto the metamaterial half-space. The orientation angle is $\phi = 0$ (curve 1), $\phi = 0.1\pi$ (curve 2), and $\phi = \phi^*(\lambda)$ (curve 3). (b) The ratio D/D_∞ for these three cases.

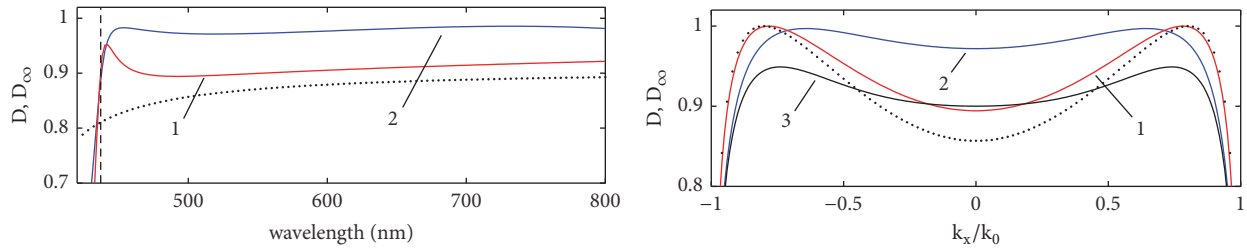

(a) (b)

FIGURE 5: (Color online) the absorption coefficient D of the nonuniform metamaterial film as a function of the (a) wavelength (at normal incidence) and (b) tangential wavevector component of the incident light ($\lambda = 500$ nm); the thickness of the film is $L_y = 200$ nm (curve 1), $L_y = 100$ nm (curve 2), and $L_y = 50$ nm (curve 3). Dotted line is the absorption coefficient D_∞ of the metamaterial half-space.

approximation it is not necessary to use continuous wires. Elongated silver particles (meta-atoms) can serve as a metallic component of the MM. Such meta-atoms suspended in a viscous liquid can be easily aligned by means of constant electric field in order to create the proper orientational pattern [30, 31].

Bearing in mind this possible realization of such an inhomogeneous metamaterial, further we demonstrate considerable enhancement of the radiation absorption in the film with spatially varying orientation of the optical axes. As before, we use in analysis the effective medium approximation.

In our simulation we use transfer-matrix method. The whole MM layer is formally split into the set of uniform sublayers with the components of inverse permittivity tensor $\widehat{\sigma} \equiv \widehat{\varepsilon}^{-1}$ locally depending on the tilt angle ϕ as

$$\begin{aligned} \sigma_{xx} &= \frac{\cos^2\phi}{\varepsilon_{xx}} + \frac{\sin^2\phi}{\varepsilon_{yy}}, \\ \sigma_{xy} &= \cos\phi \sin\phi \left(\frac{1}{\varepsilon_{xx}} - \frac{1}{\varepsilon_{yy}} \right), \\ \sigma_{yy} &= \frac{\sin^2\phi}{\varepsilon_{xx}} + \frac{\cos^2\phi}{\varepsilon_{yy}}, \end{aligned} \tag{2}$$

where ε_{xx} and ε_{yy} are the principal-axes components of the permittivity tensor. The magnetic field $\mathbf{H} \equiv \mathbf{z}_0 H$ is locally governed by the equation

$$\begin{aligned} &\frac{\partial}{\partial x}\left(\sigma_{yy}\frac{\partial H}{\partial x}\right) - \frac{\partial}{\partial x}\left(\sigma_{xy}\frac{\partial H}{\partial y}\right) - \frac{\partial}{\partial y}\left(\sigma_{xy}\frac{\partial H}{\partial x}\right) \\ &\quad + \frac{\partial}{\partial y}\left(\sigma_{xx}\frac{\partial H}{\partial y}\right) + k_0^2 H = 0, \end{aligned} \tag{3}$$

and in each sublayer it can be represented as a sum of up- and downpropagating (along the plus- and minus-y direction) waves. The relation between the amplitudes of these waves in the neighboring sublayers is found from the continuity of tangential components of electric end magnetic fields. The thickness dy of these sublayers is the step of numerical discretization, and as such, the resulting reflection and absorption coefficients do not depend on dy (i.e., the calculations with $dy/2$ and the same total thickness of the film give only small corrections to R and D).

The transfer matrix is obtained as a result of successive application of this procedure. Using the boundary conditions at the first and last sublayers we find the required reflection coefficient.

The results shown below are obtained assuming that the orientational angle increases as $\phi = (\pi/2)\, y/L_y$ ($0 \le y \le L_y$). Figure 5(a) demonstrates the wavelength dependence of the absorption coefficient $D(\lambda)$ for the nonuniform MM films with the thickness $L_y = 200$ and 100 nm. The results for thicker film are close to the case of the MM half-space, $D \approx D_\infty$. The absorption coefficient in the case of $L_y = 100$ nm is even more than D_∞ due to the interference of the incident wave and the wave which is reflected from the substrate and

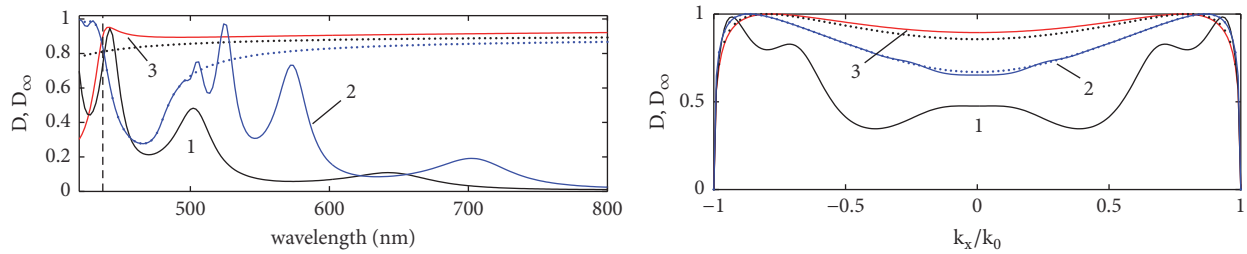

FIGURE 6: (Color online) the absorption coefficient D of the nonuniform metamaterial film (curve 3) compared with MM layer with the fixed optical axis orientation (curves 1 and 2 correspond to $\phi = 0$ and $\phi = 0.1\pi$): (a) as a function of the wavelength (at normal incidence) and (b) as a function of the tangential wavevector component of the incident light ($\lambda = 500$ nm); the thickness of the film is $L_y = 200$ nm. Dotted lines show the absorption coefficient D_∞ of the metamaterial half-space $\phi = 0$ and $\phi = 0.1\pi$.

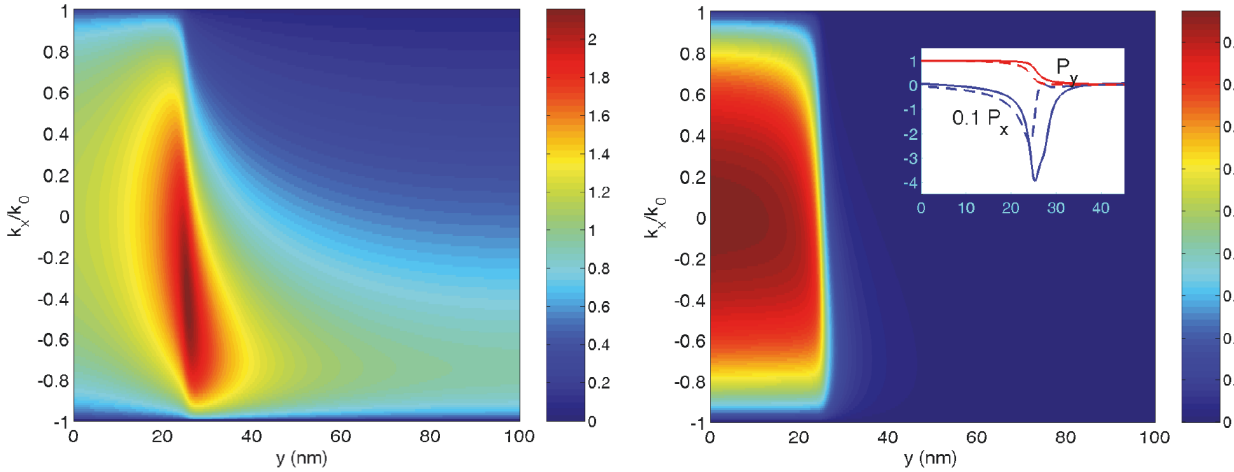

FIGURE 7: (Color online) (a) magnetic field pattern $|H_z|(y, k_x/k_0)$ for the nonuniform metamaterial film of finite thickness $L_y = 100$ nm; (b) the y component of Poynting vector, $P_y(y, k_x/k_0)$. x and y components of Poynting vector; $P_x(y)$ and $P_y(y)$ are plotted in the inset for $k_x/k_0 = -0.4$ (solid lines) and $k_x/k_0 = 0.4$ (dashed lines). Near the resonance point ($y \approx 25$ nm) P_x is tens of times higher than P_y, and the energy flows mainly in the opposite x direction. The radiation wavelength is 500 nm.

not completely damped. This interference effect results in better absorbance of the film, and the broadband character of the absorption is preserved.

The dependence of reflection and absorption on the incident angle is also an important characteristic of proposed nonuniform film, and Figure 5(b) demonstrates this function for specific wavelength $\lambda = 500$ nm and three values of the film thickness $L_y = 100$ nm (curve 1), $L_y = 200$ nm (curve 2), and $L_y = 50$ nm (curve 3, see comments below). When the component k_x of the wavevector of the incident light along the air-MM interface tends to its maximum $k_0 = 2\pi/\lambda$ the reflection sharply increases, but this is a common feature, e.g., for the reflection from dielectric half-space.

The improved absorption and broadband functionality of the proposed device are clearly seen in Figure 6, which shows the wavelength and incident angle dependence of the absorption coefficient calculated for the MM slab with fixed orientation of the optical axis (curves 1 and 2 correspond to $\phi = 0$ and $\phi = 0.1\pi$) and inhomogeneous hyperbolic metamaterial with ϕ linearly growing from 0 to $\pi/2$ (curve 3).

Figure 7 demonstrates magnetic field H_z (Figure 7(a)) and Poynting vector P_y (Figure 7(b)) pattern as a function on k_x and y. One can see that $|H_z|$ strongly depends on the incident angle, and this dependence is not symmetric with respect to $k_x = 0$. The asymmetry of the energy flow is apparent from the direction of the x component of Poynting vector P_x which is plotted in the inset of Figure 7(b), and the energy flow is mainly antialigned with the x-axis. It should be noted that, in spite of this asymmetry, the absorption coefficient $D(k_x)$ is symmetric as a function of k_x (see Figure 5(b)), and the both positive and negative k_x harmonics can be effectively absorbed.

Another important feature of the Poynting-vector pattern is its strong spatial localization. It is clear from Figure 7 that the main processes (reflection and absorption) take place in the first one-third of the film, and it seems that similar results could be achieved with half the film thickness. However, if we

place the perfectly reflecting substrate at $y = 50$ nm and keep the MM structure unchanged (such that the orientation angle varies from 0 to $\pi/4$), then the absorption of the incident wave is noticeably decreased, and the absorption coefficient takes values close to $D_{\infty}(k_x)$ (see curve 3 in Figure 5(b)).

5. Conclusion

In conclusion, we have proposed the design of an absorbing film made of nonuniform hyperbolic metamaterial. In the film with smoothly changing orientation of the optical axis from parallel to normal to the interface, the resonance absorption takes place for each wavelength with only the position of the resonance shifted. This results in broadband operation of the absorber and also its weaker sensitivity to the incident angle. The analysis based on effective medium approximation shows that a 200-nanometer-thick film operates as a metamaterial absorbing half-space. The realization of the proposed idea in optics seems to be complicated. On the other hand, the development of nanotechnology has already led to the emergence of complicated metamaterial structures, such as flexible hyperbolic metamaterial the deformation of which evidently causes *inhomogeneous orientation of the optical axis* [32]. A method of growing tilted nanowires array [33] should be also noted.

Data Availability

All the essential data is provided in either the article or the references.

Conflicts of Interest

The authors declare that there are no conflicts of interest regarding the publication of this paper.

Acknowledgments

This research is supported in part by Russian Foundation for Basic Research Grants no. 17-02-00281 and no. 16-02-00556.

References

[1] A. Poddubny, I. Iorsh, P. Belov, and Y. Kivshar, "Hyperbolic metamaterials," *Nature Photonics*, vol. 7, no. 12, pp. 948–957, 2013.

[2] D. Lu and Z. Liu, "Hyperlenses and metalenses for far-field super-resolution imaging," *Nature Communications*, vol. 3, article no. 1205, 2012.

[3] I. V. Iorsh, I. S. Mukhin, I. V. Shadrivov, P. A. Belov, and Y. S. Kivshar, "Hyperbolic metamaterials based on multilayer graphene structures," *Physical Review B: Condensed Matter and Materials Physics*, vol. 87, no. 7, Article ID 075416, 2013.

[4] Y. Guo, C. L. Cortes, S. Molesky, and Z. Jacob, "Broadband super-Planckian thermal emission from hyperbolic metamaterials," *Applied Physics Letters*, vol. 101, no. 13, Article ID 131106, 2012.

[5] S. M. Hashemi and I. S. Nefedov, "Wideband perfect absorption in arrays of tilted carbon nanotubes," *Physical Review B: Condensed Matter and Materials Physics*, vol. 86, no. 19, Article ID 195411, 2012.

[6] I. S. Nefedov, C. A. Valagiannopoulos, S. M. Hashemi, and E. I. Nefedov, "Total absorption in asymmetric hyperbolic media," *Scientific Reports*, vol. 3, article no. 2662, 2013.

[7] I. S. Nefedov, C. A. Valagiannopoulos, and L. A. Melnikov, "Perfect absorption in graphene multilayers," *Journal of Optics*, vol. 15, no. 11, Article ID 114003, 2013.

[8] S. V. Zhukovsky, O. Kidwai, and J. E. Sipe, "Physical nature of volume plasmon polaritons in hyperbolic metamaterials," *Optics Express*, vol. 21, no. 12, pp. 14982–14987, 2013.

[9] L. Ferrari, D. Lu, D. Lepage, and Z. Liu, "Enhanced spontaneous emission inside hyperbolic metamaterials," *Optics Express*, vol. 22, no. 4, pp. 4301–4306, 2014.

[10] J. Yao, Z. Liu, Y. Liu et al., "Optical negative refraction in bulk metamaterials of nanowires," *Science*, vol. 321, no. 5891, p. 930, 2008.

[11] A. J. Hoffman, L. Alekseyev, S. S. Howard et al., "Negative refraction in semiconductor metamaterials," *Nature Materials*, vol. 6, no. 12, pp. 946–950, 2007.

[12] Z. Jacob, L. V. Alekseyev, and E. Narimanov, "Optical hyperlens: far-field imaging beyond the diffraction limit," *Optics Express*, vol. 14, no. 18, pp. 8247–8256, 2006.

[13] J. Sun, M. I. Shalaev, and N. M. Litchinitser, "Experimental demonstration of a non-resonant hyperlens in the visible spectral range," *Nature Communications*, vol. 6, article no. 7201, 2015.

[14] T. U. Tumkur, L. Gu, J. K. Kitur, E. E. Narimanov, and M. A. Noginov, "Control of absorption with hyperbolic metamaterials," *Applied Physics Letters*, vol. 100, no. 16, Article ID 161103, 2012.

[15] T. U. Tumkur, J. K. Kitur, B. Chu et al., "Control of reflectance and transmittance in scattering and curvilinear hyperbolic metamaterials," *Applied Physics Letters*, vol. 101, no. 9, Article ID 091105, 2012.

[16] Z. Liu, H. Lee, Y. Xiong, C. Sun, and X. Zhang, "Far-field optical hyperlens magnifying sub-diffraction-limited objects," *Science*, vol. 315, no. 5819, p. 1686, 2007.

[17] K. Mantel, D. Bachstein, and U. Peschel, "Perfect imaging of hypersurfaces via transformation optics," *Optics Expresss*, vol. 36, no. 2, pp. 199–201, 2011.

[18] H. N. Krishnamoorthy, Z. Jacob, E. Narimanov, I. Kretzschmar, and V. M. Menon, "Topological transitions in metamaterials," *American Association for the Advancement of Science: Science*, vol. 336, no. 6078, pp. 205–209, 2012.

[19] Y. Guo, C. L. Cortes, S. Molesky, and Z. Jacob, "Broadband super-Planckian thermal emission from hyperbolic metamaterials," *Applied Physics Letters*, vol. 101, no. 13, Article ID 131106, 2012.

[20] S.-A. Biehs, M. Tschikin, and P. Ben-Abdallah, "Hyperbolic metamaterials as an analog of a blackbody in the near field," *Physical Review Letters*, vol. 109, no. 10, Article ID 104301, 2012.

[21] I. S. Nefedov and C. R. Simovski, "Giant radiation heat transfer through micron gaps," *Physical Review B: Condensed Matter and Materials Physics*, vol. 84, no. 19, Article ID 195459, 2011.

[22] Y. Cui, J. Xu, K. Fung et al., "Ultrabroadband light absorption by a sawtooth anisotropic metamaterial slab," *Nano Letters*, vol. 12, no. 3, pp. 1443–1447, 2012.

[23] H. Hu, D. Ji, X. Zeng, K. Liu, and Q. Gan, "Rainbow Trapping in Hyperbolic Metamaterial Waveguide," *Scientific Reports*, vol. 3, article 1249, 2013.

[24] Z. Jacob, J. Kim, G. V. Naik, A. Boltasseva, E. E. Narimanov, and V. M. Shalaev, "Engineering photonic density of states using metamaterials," *Applied Physics B: Lasers and Optics*, vol. 100, no. 1, pp. 215–218, 2010.

[25] P. Shekhar, J. Atkinson, and Z. Jacob, "Hyperbolic metamaterials: fundamentals and applications," *Nano Convergence*, vol. 1, no. 1, 2014.

[26] N. A. Zharova and A. A. Zharov, "Electromagnetic surface waves in liquid metacrystals," *Journal of the Optical Society of America B: Optical Physics*, vol. 33, no. 4, pp. 594–602, 2016.

[27] E. E. Narimanov, H. Li, Y. A. Barnakov, T. U. Tumkur, and M. A. Noginov, "Reduced reflection from roughened hyperbolic metamaterial," *Optics Express*, vol. 21, no. 12, pp. 14956–14961, 2013.

[28] L. Ferrari, C. Wu, D. Lepage, X. Zhang, and Z. Liu, "Hyperbolic metamaterials and their applications," *Progress in Quantum Electronics*, vol. 40, pp. 1–40, 2015.

[29] https://www.refractiveindex.info.

[30] A. A. Zharov and N. A. Zharova, "Liquid metacrystals," *Journal of the Optical Society of America B: Optical Physics*, vol. 31, no. 3, pp. 559–564, 2014.

[31] A. A. Zharov, A. A. Zharov, and N. A. Zharova, "Spontaneous reorientations of meta-atoms and electromagnetic spatial solitons in a liquid metacrystal," *Physical Review E: Statistical, Nonlinear, and Soft Matter Physics*, vol. 90, no. 2, Article ID 023207, 2014.

[32] T. Tumkur, G. Zhu, P. Black, Y. A. Barnakov, C. E. Bonner, and M. A. Noginov, "Control of spontaneous emission in a volume of functionalized hyperbolic metamaterial," *Applied Physics Letters*, vol. 99, no. 15, Article ID 151115, 2011.

[33] J. Zúñiga-Pérez, A. Rahm, C. Czekalla, J. Lenzner, M. Lorenz, and M. Grundmann, "Ordered growth of tilted ZnO nanowires: Morphological, structural and optical characterization," *Nanotechnology*, vol. 18, no. 19, Article ID 195303, 2007.